J.Serb.Chem.Soc. 70 (1) 87–95 (2005)
JSCS – 3251

UDC 549.517.1:548.2
Original scintefic paper

The growth of ruby single crystals

ALEKSANDAR GOLUBOVIĆ[1,*, #], SLOBODANKA NIKOLIĆ[1], STEVAN ĐURIĆ[2] and ANDREJA VALČIĆ[3]

[1]*Institute of Physics, Pregrevica 118, P. O. Box 68, 11080 Zemun,* [2]*Faculty of Mining and Geology, Djušina 7, P. O. Box 162, 11000 Belgrade,* [3]*Faculty of Technology and Metallurgy, Karnegijeva 4, Belgrade, Serbia and Montenegro (e-mail: galek@eunet.yu)*

(Received 9 March, revised 2 June 2004)

Abstract: Ruby (Cr:Al_2O_3) single crystals were grown by the Czochralski technique in an argon atmosphere. The critical crystal diameter d_c = 1.0 cm and the critical rate of rotation ω_c = 20 rpm were calculated by equations of the hydrodynamics of the melt. The rate of crystal growth was experimentally obtained to be 2.7 mm/h. For chemical polishing, conc. H_3PO_4 at 593 K for an exposure of 3 hours was determined. Conc. H_3PO_4 at 523 K for an exposure of 3 h was found to be a suitable etching solution. The lattice parameters a = 0.47627(6) nm and c = 1.301(1) nm were determined by X-ray powder diffraction. The obtained results are discussed and compared with published data.

Keywords: Czochralski technique, ruby, growth, single crystal, etching.

INTRODUCTION

Ruby is the red variety of corundum, the second hardest natural mineral known to mankind. The red colour of ruby is caused by trace amounts of the element chromium (0.05 % wt.) and it has been found that trivalent chromium ions played a central role in the development of solid-state lasers.[1] The first successfully optical laser constructed by Maiman consisted of a ruby crystal surrounded by a helicoidally flash tube enclosed within a polished aluminum cylindrical cavity cooled by forced air. Nelson and Boyle constructed a continuous lasing ruby by replacing the flash lamp with an arc lamp. The ruby laser has became one of the most important lasers for numerous applications, such as stimulated emission of microwave phonons (SEMP),[4] florescence line narrowing (FLN) for examination of the dynamics of non-equilibrium phonons,[5,6] fiber temperature sensors[7,8] in dermatology for the treatment of congenital melanocytic nevus,[9] removal of tattoos,[10,11] *etc*.

* Corresponding author.

Serbian Chemical Society active member.

The shape of the melt/crystal interface is strongly affected by internal radiant heat transfer through the crystal and this mechanism promotes deeply deflected interfaces toward the melt.[12] The deep interfaces in these systems can lead to detrimental features in the grown crystal. Applying both theoretical and experimental investigations, we successfully obtained many oxide single crystals, such as sapphire,[13] Nd:YAG,[14] $LiNbO_3$,[15–17] Nd:$CaWO_4$,[18] $Bi_{12}SiO_{20}$,[19,20] and $Bi_{12}GeO_{20}$.[21,22] In previous experiments,[23] Cr:Al_2O_3 single crystal were obtained despite taking some hydrodynamics equations into account. The ruby single crystals are well-known materials, but the latest applications require the production of high-quality single crystals. The aim of the present research was, besides determining the experimental conditions leading to a flat interface, to obtain Cr:Al_2O_3 single crystals in a similar way as was used for the production of other high-quality laser materials, sapphire[13] and Nd:YAG.[14]

EXPERIMENTAL

Ruby single crystals (Cr:Al_2O_3) were grown by the Czochralski technique using a MSR 2 crystal puller, as described previously.[15] The atmosphere used was argon. The starting materials were powdered Al_2O_3 (Koch & Light), Cr_2O_3 (Koch & Light) and ZrO_2 (Koch & Light) for isolation, all of 4N purity. The purity of the argon (Tehnogas) was also 4N. The iridium crucible (4 cm diameter, 4 cm high) was placed into an alumina vessel surrounded by ZrO_2 wool isolation. Double walls were used to protect the high radiation. To decrease the radial temperature gradient in the melt, alumina was mounted around all the system. The crystal rotation rates were between 20 and 50 rpm. The best results were obtained with a crystal rotation of 20 rpm. The rate of crystal growth was between 2–12 mm/h, and experimentally the best results was obtained with 2.7 mm/h. The crucible was not rotated during the growth. After the growth run, the crystal boule was cooled at a rate of about 50 K/h down to room temperature.

A solution of H_3PO_4 at 593 K with an exposure time of 3 h was found to be suitable for chemical polishing. A solution of 85 % H_3PO_4 at 523 K with an exposure time of 3 hours was found to be a suitable etching solution.

All the obtained crystal plates were observed in polarised light to reveal striations.

The chemical compositions of the products were determined by the XRD powder technique. All the samples were examined under the same conditions, using a Philips PW 1729 X-ray generator, a Philips 1710 diffractometer and the original APD software. The radiation source was an X-ray LLF tube with copper radiation and a graphite monochromator. The radiation was $\lambda CuK\alpha_1$ = 0.15405 nm. The anode tube load was 40 kV and 30 mA. Slits of 1.0 and 0.1 mm were fixed. The samples were pressed into standard aluminium frames and measured in the 2θ ranges from 10º to 120º. Each 1/50° (0.02º) was measured for 0.5 s. The MPDS program and JCPDS (ASTM) card files were used for production identification.

RESULTS AND DISCUSSION

Ruby is the standard example of a specific example of a strong-field Cr^{3+} laser material. The host crystal is α-phase corundum, generally referred to as sapphire. The plane of the oxygen ions is almost hexagonal close-packed. However, the angular distortion of some of the oxygen bonds prevents perfect close-packing, resulting in a $R\bar{3}c$ space gropu for the crystal.[1] The aluminium ions fit between the oxygen planes with an A-B-C stacking with every third cation site along the *c* axis being vacant.

The Cr^{3+} ions enter the host lattice substitutionally for the Al^{3+} ions with little size distortion and no charge mismatch. They are surrounded by six oxygen nearest-neighbour ions in almost octahedral coordination. Thus, the local site symmetry can be approximated by the O_h point group. However, the oxygen octahedron is sterched along the threefold axis[1] (corresponding to the *c* axis of the crystal) producing a trigonal distortion that lowers the site symmetry to C_{3v}. The angular displacement of the oxygen bonds further lowers the symmetry C_3. The concentration of chromium doping for standard ruby laser crystal is of the order of 0.05 wt.% (1.58×10^{19} cm^{-3}).

Oxide single crystals, such as yttrium aluminium garnet, ruby and lithium niobate, are utilized as solid-state laser hosts and as materials for acoust-opt-electronic devices, and are commonly grown by the Czochralski (CZ) method. For the production of a perfect oxide single cystal by the CZ method, it is important to acquire accurate information about the heat and mass transfer in the melt and through the phase boundaries. In the CZ crystal growth of oxides, it is well known that the melt crystal interface changes abruptly from convex to concave toward the melt as the crystal rotation rate or crystal diameter increases. This abrupt change, called "interface inversion", is considered to be caused by the change of the dominant melt flow near the interface from free convection to forced convection driven by the crystal rotation. Therefore, the relation between the melt convection and interface inversion has been investigated numerically in many previous works[24–27] because the shape of the interface inversion during the crystal growth is closely related to the crystal quality.

The hydrodynamics of a melt are governed by buoyancy-driven convection or free convection, by forced convection due to crystal rotation, and by thermo-capillary surface convection. Three dimensionless numbers can describe all these flows: Grashof (*Gr*), Reynolds (*Re*) and Marangoni (*Ma*) numbers. It can be said that the depth of the melt influences the Grashof number, the rotation rate of the crystal modifies the Reynolds number, and the temperature gradients over the surface of the melt acts on the Marangoni number.[28] Several growth parameters can be modified simultaneously to obtain a change in the hydrodynamics of the melt.

The crucible is considered to be stationary, during crystal rotation at a constant rate. Tangential stresses generated by surface tension gradients are applied to account for Marangoni flow, while no flow is allowed normal to the melt meniscus. Conduction and convection caused pulling are included in the crystal and rod pull rod. To simplify the current analysis, it was decided to neglect the effects of internal radiation through the crystal. As has been pointed out by different authors,[29,30] the crystal rotation rate and the axial temperature distribution are two very important parameters which affect the shape of the interface. Both of them are critical parameters which drastically modify the *Re* and *Gr* numbers, respectively. Therefore, these two growth parameters must be taken into account in order to understand the

shape of the interface. The *Ma* number does not change significantly if a small temperature gradient exists over the surface of the melt, and so the hydrodynamics will be governed mainly by the *Re* and *Gr* numbers. Also, it was found[31] that Marangoni natural convection is important in the case of a low Prandtl (*Pr*) number, while oxide materials have a large *Pr*.[27] Marangoni number can be written as:

$$Ma = -(\partial\gamma/\partial T)\cdot\Delta T\,(R_{\text{cruc.}} - R_{\text{crys.}})(\rho\,\nu\,\alpha)^{-1} \tag{1}$$

where $(\partial\gamma/\partial T)$ – temperature coefficient of surface tension; ΔT – temperature difference ($T_{\text{crucible}} - T_{\text{mp}}$); $R_{\text{cruc.}}$ – the crucible radius; $R_{\text{crys.}}$ – the crystal radius; ρ – the melt density; ν – the kinetic viscosity, and α – the thermal diffusivity of the melt.

Reynolds and Grashof numbers can be written as:

$$Re = \omega\, r^2\, \nu^{-1} \tag{2}$$

$$Gr = g\,\beta\,\Delta T\, R^3\, \nu^{-2} \tag{3}$$

where ω – rotation rate; r – crystal radius, ν –kinematic viscosity; g – acceleration due to gravity, β – volumetric expansion coefficient of the melt, ΔT – temperature difference ($T_{\text{crucible}} - T_{\text{mp}}$), and R – radius of the crucible. It was presumed, as did Carruthers,[32] that the kinematic viscosity at the melt/crystal interface did not change during the growth process and that there was equilibrium $Gr = Re^2$. There is, during this time, a flat melt/crystal interface with a critical rotation rate ω_c and a critical diameter α_c. It was decided to use the relations derived by Carruthers in the calculations for our experimental system. These relations are in a good agreement with the experimental data of many authors[29,30,33] for crystals with a high Prandtl number and it was assumed that they could also be useful in our case. In this way, by applying the hydrodynamic forms, the values of the critical rate of rotation, ω_c = 20 rpm, and the critical diameter, d_c = 10 mm, were obtained. The rate of crystal growth was experimentally obtained to be 2.7 mm/h. The coefficient of the Cr^{3+} distribution in the Al_2O_3 is 1. A cone angle of ≈ 60º was used for the growth of the $Cr:Al_2O_3$ single crystal growth, which was an empirical value no appropriate value could be found in the literature.

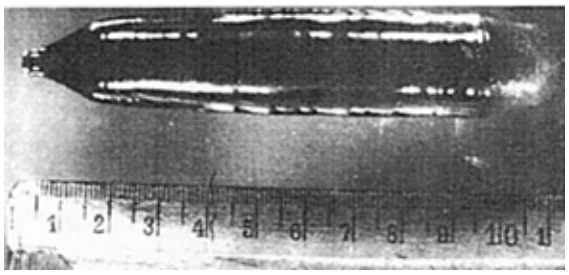

Fig. 1. A view of an obtained ruby single crystal.

An obtained ruby single crystal is shown in Fig. 1. The concentration of Cr^{3+} in the ruby was 0.05 wt.%. A plate of a ruby single crystal is shown in Fig. 2.

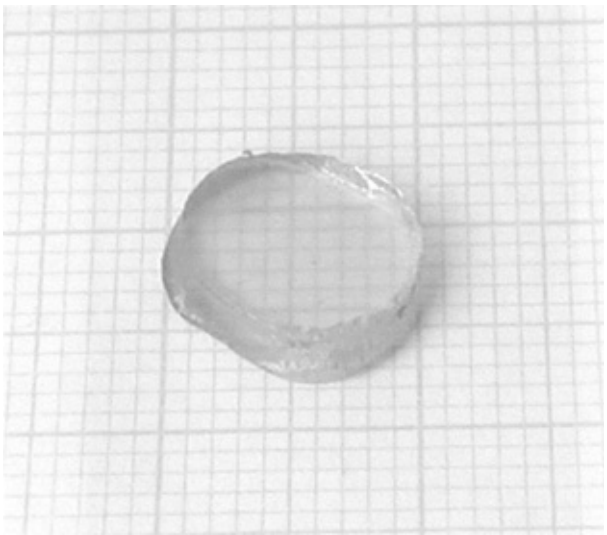

Fig. 2. A view of a chemically polished ruby single crystal plate.

At temperatures higher than 1300 K, iridium decomposes. Ruby has a high melting point (2323 K) and IrO_2 from the iridium crucible decomposes to metalic Ir which falls into the melt and is incorporated into the growing crystal. The consequences are particles of 1–5 μ which scatter light and form large striations.[34] This problem was solved by flowing argon which carried away the iridium from the crystal growth zone. Some authors used Mo crucible to solve this problem[35] as the maximum of temperature for an Ir crucible is 2423 K (melting point 2725 K) compared to 2573 K for a Mo crucible (melting point 2893 K).

The ruby single crystals were cut, chemically polished in conc. H_3PO_4 at 593 K for 3 h and etched in conc. H_3PO_4 at 523 K for 3 h. The average number of dislocations was 5×10^2 cm^{-2}. The obtained etch-pits had the same shape as if material was the single crystals. In our previous studies the average number of dislocations were $1.5–2.0\times10^4$ cm^{-2},[23,36] but in those experiments on crystal growth, the hydrodynamic equations were not taken into consideration. The thermal stresses have a minimum value near a critical Reynolds number at which the melt/crystal interface occurs,[37] and for this reason the dislocation density was smaller. It has been found[38] that sapphire wafers can be chemically polished and thinned in molten borax (1223–1323 K), and chemically etched in molten borax (1123–1273 K) in about 15 min. In this work molten borax was not used for polishing and etching as preference was given to the lower temperature processes.

The polished crystal plates observed under polarised light showed the absence of bubbles, entrapments, non-homogeneous impurity concentrations and striations.

The structure properties were obtained using X-ray analysis of powdered samples. A Philips PW 1710 diffractometer was used in the 2θ range from 10º to 120º The unit cell of ruby was calculated by the least square method using 15 reflections

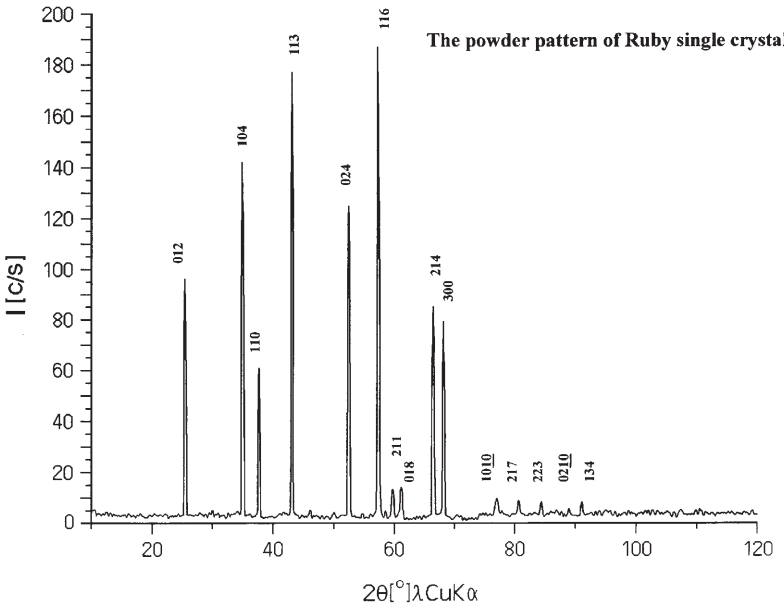

Fig. 3. X-Ray pattern of powdered ruby single crystal.

including an additional five $K\alpha_2$ reflections. All reflections corresponded to Al_2O_3 crystals with the parameters of the rhombohedral unit cell being $a = 0.47592(1)$ nm and $c = 1.2992(3)$ nm.[39] Some divergence from the compared results can be explained by the fact that X-ray powder diffraction analysis gives a statistical result. Our calculated results for the lattice parameters are $a = 0.47627(6)$ nm and $c = 1.301(1)$ nm, which are in good agreement with published data.[1,5,40] The X-ray difractogram for powdered ruby is given in Fig. 3, in which the weak reflections are not marked with Mueller indices.

The intensities of the reflections for some crystal planes, together with their Mueller indices and distances between the planes of the reflections are given in Table I. The intensities of the reflections from Fig. 3 are given together with intensities for the same planes published in JCPDS ("Joint Committee on Powder Diffraction Standards").

TABLE I. The spacing of the lattice planes, Mueller indices and intensities for ruby ($Cr:Al_2O_3$) together with literature data[39] for comparison

2θ/°	$2\theta_c$/°	d/nm	d_c/nm	(hkl)	I/I_0	$(I/I_0)_c$
25.578	25.530	0.34797	0.34863	012	45	53
35.150	35.065	0.25508	0.25569	104	98	62
37.767	37.582	0.23794	0.23814	110	44	29
43.340	43.265	0.20853	0.20896	113	100	90
52.548	52.480	0.17400	0.17421	024	48	60
	52.620		0.17418			32

TABLE I. Continued

2θ/°	$2\theta_c$/°	d/nm	d_c/nm	(hkl)	I/I_0	$(I/I_0)_c$
57.498	57.428	0.16015	0.16034	116	96	100
	57.581		0.16030			50
59.738	59.700	0.15466	0.15475	211	3	8
	59.860		0.15432			4
61.303	61.288	0.15110	0.15121	018	9	9
66.514	66.450	0.14015	0.14058	214	38	44
	66.640		0.14056			20
68.202	68.145	0.13737	0.13749	300	27	32
	68.340		0.13748			16
76.873	76.866	0.12391	0.12379	$10\underline{1}0$	17	3
80.415	80.406	0.11931	0.11907	217	1	3
84.348	84.339	0.11472	0.11476	223	5	3
88.997	88.990	0.10990	0.10803	$02\underline{1}0$	8	2
91.179	91.171	0.09802	0.09806	134	10	3

It should also be mentioned that doublets were found for (hkl): 024, 116, 211, 214 and 300 which correspond to X-ray reflections of $K\alpha_1$ and $K\alpha_2$, present in the ratio 2:1.[41] It has been reported that only almost perfect single crystals can split X-ray reflections into $K\alpha_1$ and $K\alpha_2$ and the presence of doublets is one more confirmation of the high quality of the obtained crystals. It also confirmed our assumption about the Marangoni number as rotation shows a tendency to weaken the Marangoni effect, at lower rotation rates, it prevents the surface spoke pattern structure from penetrating into the melt.[42]

CONCLUSION

The conditions for growing ruby single crystals were calculated by using a combination of Reynolds and Grashof numbers. From the hydrodynamics of the melt a critical crystal diameter d_c = 1.0 cm and a critical rate of rotation ω_c = 20 rpm were calculated. The value of the rate of crystal growth was experimentally found to be 2.7 mm/h.

Conc. H_3PO_4 was found to be a suitable solution for both polishing and etching.

Acknowledgement: This work is supported by Serbian Ministry of Science and Environmental Protection under the Project No. 1481.

ИЗВОД

РАСТ МОНОКРИСТАЛА РУБИНА

АЛЕКСАНДАР ГОЛУБОВИЋ*, СЛОБОДАНКА НИКОЛИЋ*, СТЕВАН ЂУРИЋ** и АНДРЕЈА ВАЛЧИЋ***

**Институт за физику, Прегревица 118, п. фах 68, 11080 Земун, **Рударско-геолошки факултет, Ђушина 7, п. фах 162, 11000 Београд и ***Технолошко-металуршки факултет, Карнегијева 4, 11000 Београд*

Монокристали рубина (Al_2O_4) су расли помоћу технике по Чохралском у аргону. Вредности критичног пречника d_c = 1,0 cm и критичне брзине ротације ω_c = 20 o/min су одређене помоћу једначина динамике флуида. Брзина извлачења кристала од 2,7 mm/h је одређена експериментално. Као средство зе хемијско полирање је одређена конц. H_3PO_4 на 593 K при излагању од 3 сата. Конц. H_3PO_4 на 523 K при излагању од 3 сата се показала као погодно средство за нагризање. Одређени су параметри решетке a = 0,47627(6) nm и c = 1,301(1) nm помоћу рендгенске дифрационе анализе праха. Добијени резултати су дискутовани и упоређени са литературним подацима.

(Примљено 9. марта, ревидирано 2. јуна 2004)

REFERENCES

1. R. S. Powell, *Physics of Solid-State Laser Materials*, G. W. F. Drake, Ed., Springer-Verlag, New York, Berlin, Heidelberg, 1998, pp. 215–238
2. T. H. Maiman, *Nature* **187** (1960) 493
3. D. F. Nelson, W. S. Boyle, *Appl. Opt.* **1** (1962) 181
4. E. M. Ganapolskii, D. N. Makovetskii, *Solid State Com.* **90** (1994) 501
5. M. J. van Dort, J. J. Dijkhuis, H. W. de Wijin, *Phys. Rev. B* **41** (1990) 8657
6. K. Z. Troost, M. J. van Dort, J. I. Dijkhuis, H. W. de Wijn, *Phys. Rev. B* **43** (1991) 98
7. K. T. V. Grattan, Z. Y. Zhang, T. Sun, Y. Shen, L. Tong, Z. Ding, *Measur. Sci. and Techn.* **12** (2001) 981
8. H.C. Seat, J. H. Sharp, Z. Y. Zhang, K. T. V. Grattan, *Senzors and Actuators A: Physical* **101** (2002) 24
9. J. S. Nelson, K. M. Kelly, *Derm. Surg.* **25** (1999) 274
10. R. Ruedlinger, *J. Cut. Laser Therapy* **2** (2000) 37
11. M. Kupermanbeade, V. J. Levine, R. Ashinoff, *Am. J. Clin. Derm.* **2** (2001) 21
12. Q. Xiao, J. J. Derby, *J. Crystal Growth* **139** (1994) 147
13. A. Golubović, S. Nikolić, S. Đurić, A. Valčić, *J. Serb. Chem. Soc.* **66** (2001) 411
14. A. Golubović, S. Nikolić, R. Gajić, S. Đurić, A. Valčić, *J. Serb. Chem. Soc.* **67** (2002) 291
15. A. Golubović, R. Gajić, A. Valčić, *J. Serb. Chem. Soc.* **63** (1998) 863
16. A. Golubović, S. Nikolić, R. Gajić, S. Đurić, A. Jelisijević, D. Vuković, A. Valčić, *J. Serb. Chem. Soc.* **64** (1999) 637
17. A. Golubović, R. Gajić, S. Nikolić, S. Đurić, A. Valčić, *J. Serb. Chem. Soc.* **65** (2000) 391
18. A. Golubović, S. Nikolić, R. Gajić, S. Đurić, A. Valčić, *J. Serb. Chem. Soc.* **68** (2003) 1001
19. A. Golubović, S. Nikolić, R. Gajić, S. Đurić, A. Valčić, *J. Serb. Chem. Soc.* **64** (1999) 553
20. A. Golubović, S. Nikolić, R. Gajić, S. Đurić, A. Valčić, *J. Serb. Chem. Soc.* **67** (2002) 279
21. A. Golubović, R. Gajić, C. Chen, A. Valčić, *J. Serb. Chem. Soc.* **65** (2000) 611
22. A. Golubović, R. Gajić, C. Chen, A. Valčić, *Hem. industrija* **54** (2000) 530 (in Serbian)
23. A. Valčić, R. Roknić, S. Nikolić, *Proc. XXII Symp. ETAN in Marines*, Zadar, Croatia, 1980, p. 354 (in Serbian)
24. Q. Xiao, J. J. Derby, *J. Cryst. Growth* **128** (1994) 188
25. Q. Xiao, J. J. Derby, *J. Cryst. Growth* **139** (1994) 147
26. H. Kopeusch, *J. Cryst. Growth* **102** (1990) 575
27. M. Kobayashi, T. Hagano, T. Tsukada, M. Hoyawa, *J. Cryst. Growth* **235** (2002) 258
28. M. T. Santos, J. C. Rojo, L. Arizmedni, E. Dieguez, *J. Crystal Growth* **142** (1994) 103

29. R. A. Brown, *Advances in Crystal Growth*, P. M. Dryburgh, Ed., Prentice-Hall, Englewood Cliffs, New York, 1987, p. 41
30. R. Ristorcelli, J. L. Lumley, *J. Crystal Growth* **116** (1992) 647
31. A. D. W. Jones, *J. Crystal Growth* **88** (1988) 465
32. J. R. Carruthers, *J. Crystal Growth* **36** (1976) 212
33. S. Enger, B. Basu, M. Breuer, F. Durst, *J. Crystal Growth* **219** (2000) 144
34. V. A. Borodin, V. V. Sidiriv, S. N. Rossolenko, T. A. Steriopolo, V. A. Tatarchenko, T. N. Yalovets, *J. Crystal Growth* **104** (1990) 69
35. G. M. Loiacano, *Tunable Solid State Lasers II*, P. Hamerling, A. B. Budgor, A. Pinto, Eds., Springer-Verlag, Berlin, 1985, pp. 98–104
36. A. Valčić, R. Roknić, S. Nikolić, *Proc. 23. Chem. Symp. of SR Serbia*, Belgrade, Yugoslavia, 1981, p. 627 (in Serbian)
37. M. Kobayashi, T. Tsukada, M. Hozawa, *J. Crystal Growth* **241** (2002) 241
38. Y. Qiang, D. Peinzhen, G. Fuxi, *J. Crystal Growth* **108** (1991) 377
39. JCPDS 43-1484
40. J. Guo, D. E. Ellis, D. J. Lam, *Phys. Rev. B* **45** (1992) 3204
41. S. Đurić, *Nauka Tehnika Bezbednost* **1** (1995) 45 (in Serbian)
42. C. J. Jing, N. Imashi, T. Sato, Y. Miyazawa, *J. Crystal Growth* **216** (2000) 372.